

Design and Fabrication of a Displacement Sensor Using Screen Printing Technology and Piezoelectric Nanofibers in d_{33} Mode

Yi-Chen Chen,^{1,2} Chih-Kun Cheng,³ and Sheng-Chih Shen^{1*}

¹Department Systems and Naval Mechatronic Engineering, National Cheng Kung University,
No. 1, University Road, Tainan City 701, Taiwan

²Intelligent Mechatronics Department, Smart Micro-systems Technology Center,
Industrial Technology Research Institute, Tainan City 704, Taiwan

³Department of Electrical Engineering, Far East University, Taiwan

(Received May 3, 2018; accepted October 18, 2018)

Keywords: piezoelectric nanofiber, PVDF, d_{33} mode, electrode design

Polyvinylidene fluoride (PVDF) piezoelectric nanofibers were fabricated through near-field electrospinning (NFES) to develop a flexible piezoelectric element. Innovative screen printing technology was employed to produce bend-type electrodes designed with d_{33} mode patterns. The electrodes and PVDF nanofibers were then attached to a polyimide film substrate. Compared with piezoelectric ceramics, piezoelectric fibers are inexpensive, flexible, and highly biocompatible. They also have a higher electron density than piezoelectric films, indicating that they are more efficient in electromechanical conversion. Thus, in this study, we adopted piezoelectric fibers to create a displacement sensor with bend-type electrodes that employed optimized pattern designs to increase the efficiency of piezoelectric conversion and sensitivity. The experimental results revealed that the type of electrode was critical for enhancing output voltage. The novel bend-type electrodes induced an average positive voltage of 960.5 mV during a tapping experiment, increasing the maximum voltage by 59.74% compared with a series-type electrode. The positioning accuracy of the displacement sensor was 600 μm ; thus, the sensor could successfully determine positioning, confirming the feasibility of the displacement sensing mechanism.

1. Introduction

The rapid advance of micro-electromechanical systems and semiconductor engineering in recent years has enabled the development of ever-smaller electronic components, which has led to a marked increase in the production of wearable devices. Most wearable devices are powered by batteries, but as such devices become smaller, the feasibility of using conventional batteries comes into question. In developing a new battery technology, one of the primary concerns is how sensing elements can operate at a reduced scale. Furthermore, the miniaturization of sensing elements heightens the importance of detecting minute changes, which is why

*Corresponding author: e-mail: scshen@mail.ncku.edu.tw
<https://doi.org/10.18494/SAM.2019.2083>

highly sensitive and self-powered piezoelectric materials have recently received substantial attention. The unique self-powered properties of piezoelectric materials are a result of the piezoelectric effect. A positive piezoelectric effect can convert mechanical energy applied to a piezoelectric material into electrical energy, thereby allowing the material to draw energy from its environment to form a self-powered system for mobile and wireless devices. Polymeric piezoelectric nanofibers are the most promising among the various piezoelectric materials. Unlike conventional piezoelectric ceramics, which are extremely brittle and difficult to produce, polymeric piezoelectric nanofibers are inexpensive and have excellent flexibility and biocompatibility.⁽¹⁾ Moreover, compared with piezoelectric films, piezoelectric polymers are more efficient in electromechanical energy conversion.⁽²⁾

Because of the growing demand for wireless devices and continuous sensing systems, Wang and Song used zinc oxide to fabricate piezoelectric nanowires for self-powered piezoelectric nanogenerators.⁽³⁾ They first employed the vapor–liquid–solid method to produce zinc oxide nanowire arrays—approximately 0.2–0.5 μm in length and 100–800 nm in diameter—to convert mechanical energy into electrical energy. Then, they used Kevlar fibers as a base to grow ZnO nanowire arrays approximately 3.5 μm in length and 50–200 nm in diameter; the nanowire arrays relied on the friction between fibers to generate a power output of 20–80 mW/m^2 , thereby developing prototype power-generating garments.⁽⁴⁾ One year later, they fixed ZnO nanofibers (100–500 μm in length and 100–800 nm in diameter) on a flexible substrate that could be worn on a finger, and this device was able to generate electricity (~ 25 mV and 150 pA) through the strain induced by the curling of the finger.⁽⁵⁾ Because the vapor–liquid–solid method is difficult to apply to produce nanowires greater than 50 μm in length, electrospinning techniques have been proposed as an alternative for the production of piezoelectric nanofibers. Electrospinning techniques can be divided into two categories, namely, conventional far-field electrospinning (FFES)⁽⁶⁾ and near-field electrospinning (NFES).⁽⁷⁾ Common materials for electrospinning include lead zirconate titanate (PZT) and polyvinylidene fluoride (PVDF).

Although a PZT piezoelectric nanofiber has an extremely high piezoelectric coefficient, its application in electrospinning requires it to be dissolved in a solvent, which lowers its density and energy conversion efficiency. Furthermore, to increase its piezoelectric properties, it must be annealed at temperatures above 600 $^{\circ}\text{C}$, which adds a layer of difficulty to the process. Considering that PZT contains lead, a toxic heavy metal, it is far from an ideal option. By contrast, PVDF is a typical polymeric piezoelectric material, in that it is flexible, light, impact-resistant, and easy to mold compared with most ceramic or monocrystalline piezoelectric materials; moreover, it is highly efficient in electromechanical energy conversion. These characteristics mean that PVDF has gradually begun to replace PZT and attracted substantial attention. Yee *et al.*⁽⁸⁾ were the first to apply FFES in the production of piezoelectric nanofibers with PVDF, and Hansen *et al.*⁽⁹⁾ also applied FFES to produce piezoelectric nanofibers 600 nm in diameter for integration into a biological fuel cell for an innovative energy-harvesting system. Chang and coworkers^(2,10) proposed the application of NFES in the production of PVDF piezoelectric nanofibers and experimentally proved that strain rate affects voltage and output current. Liu *et al.*⁽¹¹⁾ proposed an improved NFES method that employed a rotating glass tube collector to fabricate and collect highly aligned small-diameter piezoelectric nanofibers, and they also proposed the use of carbon nanotubes to enhance piezoelectric properties. On the

basis of the NFES technique, Pan *et al.*⁽¹²⁾ developed a close-loop motor control for a cylindrical collector to obtain continuous and uniform PVDF piezoelectric fiber arrays.

Electrospinning is the primary method of piezoelectric nanofiber production. It relies on an external electric field to attract the polymer solution to the front end of a metal spinning needle, forming a triangular cone known as the Taylor cone.⁽¹³⁾ When the voltage rises to a certain point, the charged-up solution breaks its own surface tension and jets toward a collector with an opposite polarity. The charged liquid column jetted out (cone jet) has the same polarity as the direction of the electric field. As aforementioned, electrospinning has two varieties, FFES and NFES, with the difference lying in the distance between the needle nozzle and the collector. Because the distance travelled is longer in FFES, a stronger electric field is required, which leads to the cone jet having a much higher charge density. The resultant repulsion force can induce turbulence in the cone jet, which causes the fibers to scatter arbitrarily instead of forming into orderly arrays. This can compromise the electric output because the effects of the fibers can cancel each other owing to opposite polarities. NFES was developed to overcome this shortcoming; the distance is reduced from several dozen centimeters (generally between 8 to 30 cm) to a value within 1 cm. As a result, the required strength of the electric field is reduced and the electrospun fibers are collected completely before turbulence can begin to form. However, a reduced electric field also means that the piezoelectric effect is weakened because of insufficient polarization. Therefore, FFES should be used for the precipitation of fibers over a large area; if the orderly precipitation of fibers within a small area is desired, NFES is superior.

The present study applied PVDF formed through NFES as the material for fabricating piezoelectric nanofibers, which were employed to create a flexible piezoelectric sensing element. Because a piezoelectric nanofiber is a one-dimensional linear material, strain primarily occurs along its linear axis. Therefore, the d_{33} mode was chosen for fabricating the piezoelectric sensing element and determining its electrode parameters. Parameters for the electrode design included the form, number of pairs, width, and interval of electrodes, which were optimized to enhance the energy conversion efficiency of the PVDF piezoelectric sensing element. The electrodes were produced using the screen printing method, which directly printed the metal electrodes onto polyimide films. After the electrodes were completed, the PVDF was firmly attached to the electrodes and packed with a plastic substrate to form the flexible piezoelectric sensing element. A tapping device was made to measure the output of the sensing element. The purpose of the experiment was twofold: (1) to observe how—after fixing the source of strain to ensure the input of the direct piezoelectric effects was on the same basis—the different electrode parameters affected the voltage output of the sensing element, and (2) to design and appraise a sensing module based on the piezoelectric sensing element.

2. Design and Fabrication

2.1 Electrode design

Owing to the polarity of piezoelectric materials, the IEEE compact matrix notation defines their corresponding coordinates. In this study, 1, 2, and 3 are used to denote the X -, Y -, and

Z-axes, respectively, and 4, 5, and 6 the directions of rotation around X, Y, and Z, respectively. The IEEE compact matrix notation uses dip to demonstrate the piezoelectric operating mode, where i represents the direction of the electric field and q represents the stress orientation, and it is mainly used to separate the working mode into d_{15} , d_{31} , and d_{33} mode operations (Fig. 1). Device fabrication in the d_{15} mode is challenging because the electrode does not easily collect charges; therefore, in this study the d_{31} and d_{33} modes were adopted.

Because the operating principle of piezoelectric sensing elements is derived from the piezoelectric effect, we determined the output voltage equations of piezoelectric nanofibers as

$$V_3 = g_{31}T_1H_3 + g_{32}T_2H_3 + g_{33}T_3H_3, \tag{1}$$

where V is the voltage, g is the piezoelectric voltage constant, T is the stress, and H is the electrode spacing. From this equation, electrode spacing is the factor that affects output voltage. If the electrode is configured to the d_{31} mode, changing the distance between the electrodes adjusts the thickness of the piezoelectric fibers; if the electrode is configured to the d_{33} mode, changing the distance between the electrodes only adjusts the length of the piezoelectric fibers (Fig. 2).

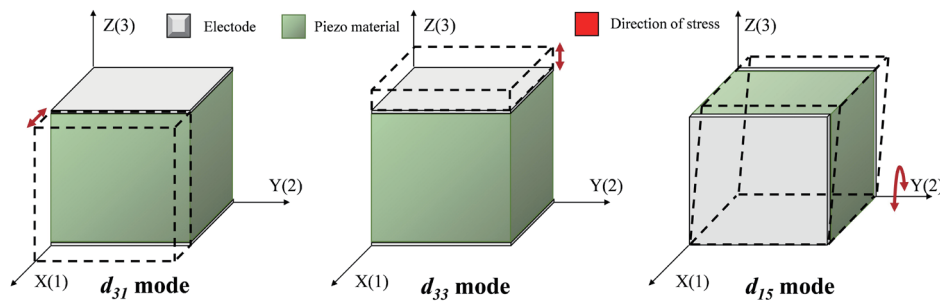


Fig. 1. (Color online) Operating modes of piezomaterial.

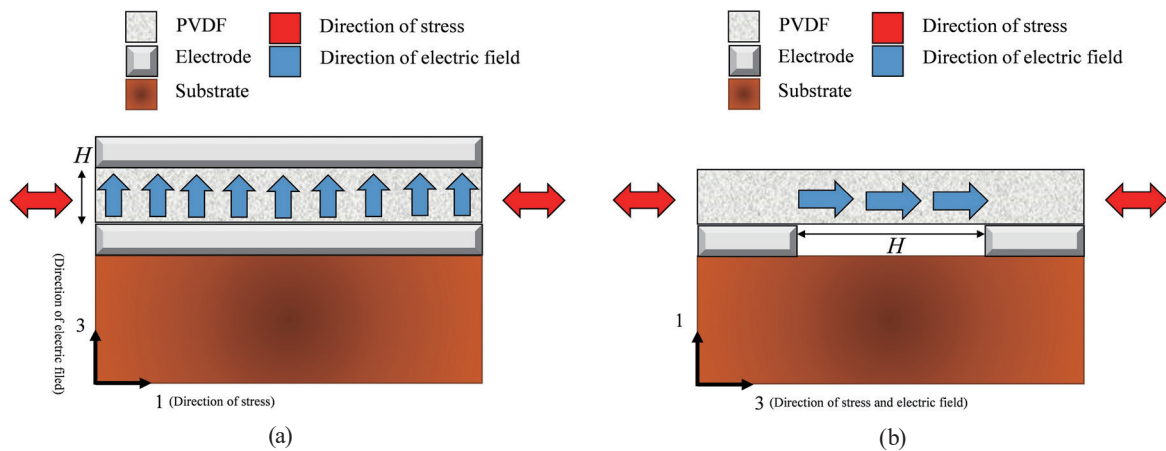


Fig. 2. (Color online) Comparison of operating modes. (a) d_{31} mode and (b) d_{33} mode.

Adjusting the length of the piezoelectric fibers is easier than adjusting their thickness and also enhances the advantages of NFES. Therefore, in this study the d_{33} mode was adopted. Thus, T_1 and T_2 in Eq. (1), which represent the nonaxial direction of the stress, are taken as zero to provide the final equation

$$V_3 = g_{33}T_3H_3. \quad (2)$$

On the basis of Eq. (2), we designed the electrode parameters including electrode width (W), electrode spacing (H), the numbers of electrode pairs (P), and electrode type (parallel or series type) (Fig. 3).

In this study, we also designed a novel bend-type electrode. Because piezoelectric sensing elements primarily use output voltage as the source for signal acquisition, the factors affecting output voltage in the piezoelectric equation indicate that series-type electrodes provide the optimal voltage output among various possible electrode configurations. However, because series-type electrodes require a large surface area, this high voltage output is achieved at the expense of device size. Consequently, in the present study, bend-type electrodes were adopted, relying on H to determine voltage output, to achieve the same results as series-type electrodes but in a smaller size (Fig. 4). The parameters used in this experiment are listed in Table 1.

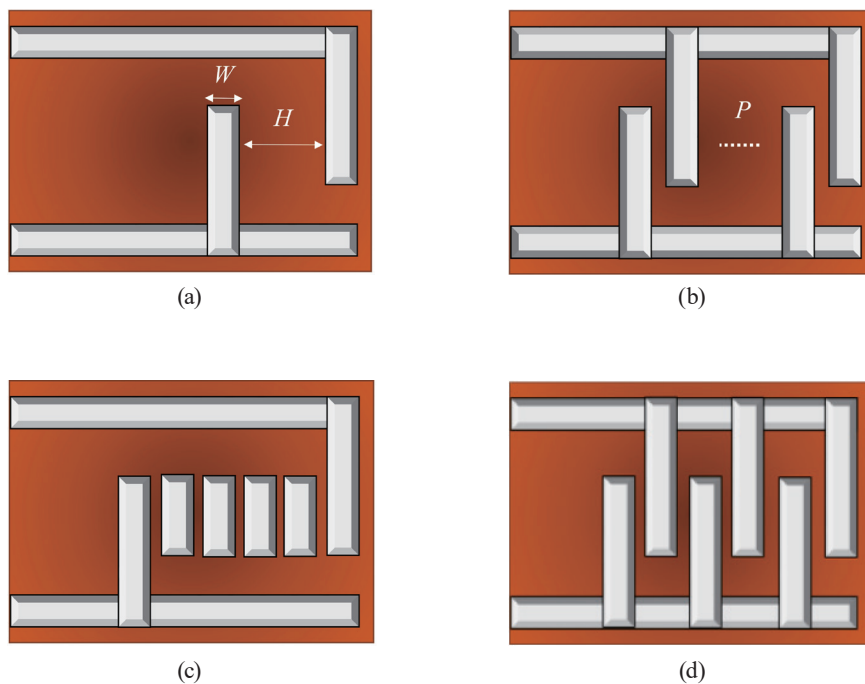


Fig. 3. (Color online) Parameters of the electrode design. (a) Width and spacing, (b) pairs, (c) parallel type, and (d) series type.

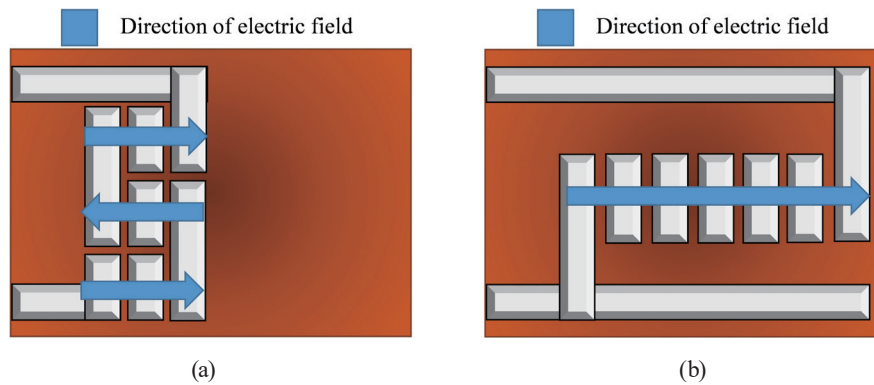


Fig. 4. (Color online) Equivalent type of electrode. (a) Bend and (b) series type.

Table 1
Electrode parameters.

Electrode type	Electrode spacing H (mm)	Electrode width W (mm)	Number of electrode pairs P
Parallel	0.0625, 0.125, 0.25, 0.5	0.125, 0.25, 0.5	1
Parallel	0.0625, 0.125, 0.25, 0.5	0.125, 0.25, 0.5	3, 5
Series	0.0625, 0.125, 0.25, 0.5	0.125, 0.25, 0.5	3, 5
Bend	0.0625, 0.125, 0.25, 0.5	0.125, 0.25, 0.5	3, 5

2.2 Sensing element

Photolithography has always been the primary production method for electrodes of piezoelectric devices. However, because of the complicated process of photolithography, the large number of parameters involved in the present study, and the requirement for steady mass production, the screen printing technology was eventually chosen because of its simplicity, low cost, and scalability. The sensing elements used in this study were produced in three steps: (1) the screen-printed electrodes were cut into predetermined geometric forms, and the PVDF was cut according to the electrode configuration; (2) the electrodes were firmly attached to the PVDF with wires connecting the larger electrodes; and (3) the sensing element was packed in a flexible plastic material to protect it from damage and improve its stability.

The PVDF used in this experiment was produced with NFES and collected using a rotating tube collector (Fig. 5). Its parameters are listed in Table 2. The crystalline phase of PVDF is mainly composed of three bonding modes, namely, the α , β , and γ phases. The α phase is the most common bond in PVDF materials before being polarized. However, the dipole moments can easily cancel each other out, because the distribution of dipole moments is random and orderless. Therefore, the α phase does not have piezoelectricity. On the contrary, the dipole moment distribution of the β phase is symmetric and orderly, which yields the piezoelectric properties. As for the dipole moment distribution pattern of the γ phase, it is the crystallization of a mixture of the α and β phases. In the electrospinning process, mechanical stretching and electric-field polarization are applied to transform various bonds inside the PVDF material into



Fig. 5. (Color online) PVDF piezoelectric nanofibers.

Table 2
Parameters for fabricating PVDF piezoelectric nanofibers.

Parameter	Parametric value
Electric field spacing	1–2 mm
Drive voltage	600–1200 V
PVDF concentration	18 wt%
Multiwalled carbon nanotube content	0–0.03 wt%
Collection rate	80–100 mm/s
Needle nozzle size	0.23 mm

the crystalline structure of the β phase gradually, thereby forming a multimolecular polymer with high piezoelectric conversion. Many factors affect the quality of PVDF fibers produced by this process, such as the size of the syringe needle, the applied voltage of the PVDF precursor solution, and the rotation speed of the drum collector. In addition, the PVDF fibers are blended by multiwalled carbon nanotubes (MWCNTs), in order to increase their piezoelectricity.

Because the electrodes used in the present study were screen-printed, the ink used should be conductive. Common conductive inks include aluminum, carbon, and silver inks: aluminum ink is usually used for electrodes in solar cells and must be baked dry at extremely high temperatures; carbon ink is the cheapest ink among the three but has the lowest conductivity whereas silver ink has the highest conductivity. Considering the requirement for high sensitivity, silver ink was chosen for fabricating the electrodes of the piezoelectric sensing element.

The production of the screen-printed electrodes consisted of three steps: (1) preparing the screen and substrate; (2) printing with the conductive ink; and (3) baking the ink dry. The finished products (screen-printed electrodes) are shown in Fig. 6(a). Subsequently, the PVDF piezoelectric nanofibers were cut according to the size of the electrodes and firmly attached to the electrodes, after which the electrodes were thermally imprinted in a plastic substrate, as in Fig. 6(b).

3. Experiment and Discussion

To determine the effect of the optimized electrodes on the output efficiency of the PVDF piezoelectric fiber, we tested the electrodes against reference values with the same level of strain. To do so, we designed a tapping device (Fig. 7) that allowed us to measure the properties

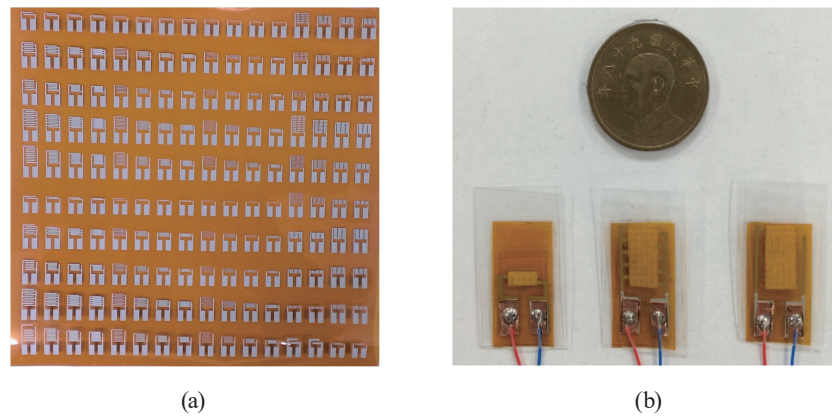


Fig. 6. (Color online) Fabrication of the piezoelectric sensing element. (a) Screen-printed electrodes and (b) sensing element.

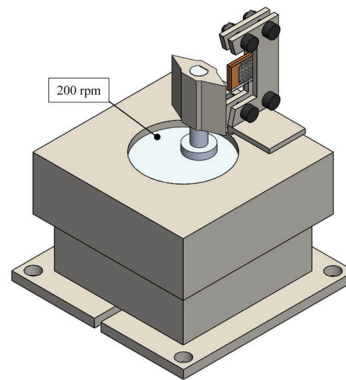


Fig. 7. (Color online) Tapping device for piezoelectric signal measurement.

of the piezoelectric sensing element. In case of noise interference during measurement, we used the switching polarity criterion to verify whether the measuring signal was the piezoelectric signal (Fig. 8).

First, we measured the mechatronic properties by fixing the electrode width ($W = 0.5$ mm). The measurement results for each parameter are plotted in Fig. 9.

The relationship between electrode width and output voltage is illustrated in Fig. 10. An electrode width of 0.5 mm provided the highest sensitivity recorded in this research, and it was thus selected for the fabrication of the bend-type electrodes, whose mechatronics properties were measured. The output voltage of the bend-type electrodes is shown in Fig. 11.

As shown in Fig. 11, the output voltage was markedly improved compared with that of the series-type electrodes, but the peak voltage was relatively unstable. This is likely because of the complex production process. Dividing the piezoelectric fibers into three parts to paste them on the substrate can lead to large errors such as those displayed in Fig. 11. The average maximum positive peak voltage of the bend-type electrodes increased 59.74% compared with that of the series-type electrodes (from 573.8 to 960.5 mV). Because of the small scale and high sensitivity of the nanopiezoelectric fiber sensing elements, we attempted to apply them to the displacement sensor. The assembly diagram is illustrated in Fig. 12.

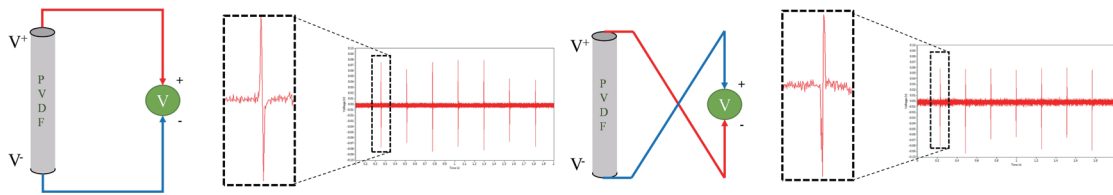


Fig. 8. (Color online) Switching polarity criterion.

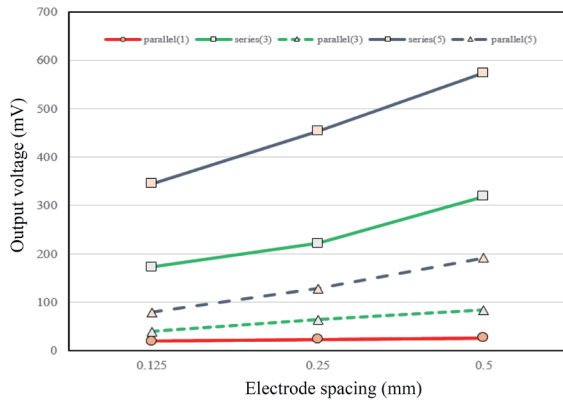


Fig. 9. (Color online) Electrode parameters and output voltage relationship (spacing).

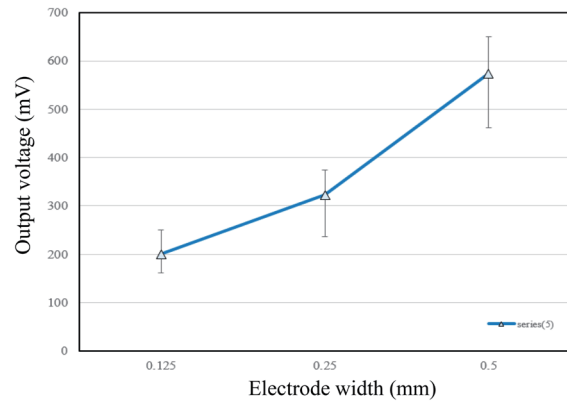


Fig. 10. (Color online) Electrode parameters and output voltage relationship (width).

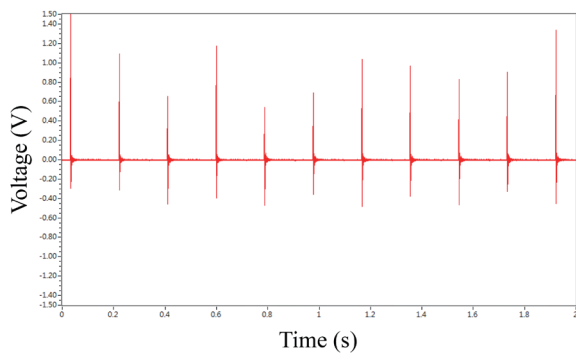


Fig. 11. (Color online) Bend-type electron voltage measurement.

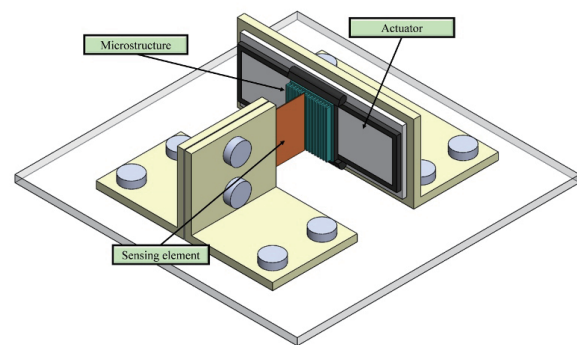
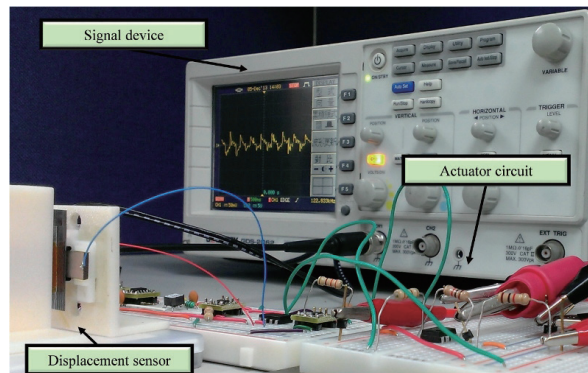
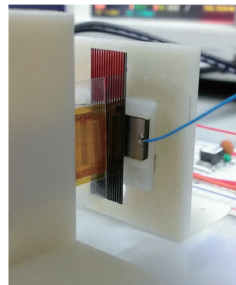


Fig. 12. (Color online) Displacement sensor assembly diagram.

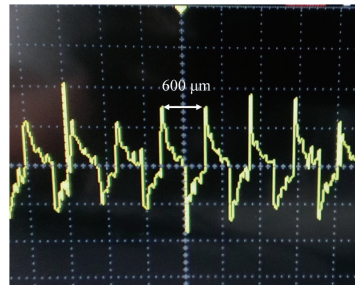
The experimental setup used to test the prototype displacement sensor is shown in Fig. 13. The pitch of the microstructure was 600 μm , and the piezoelectric signal was produced by bending the piezoelectric sensing element. Each unit of the piezoelectric signal represented an actuator displacement of 600 μm ; thus, the positioning accuracy was 600 μm . This prototype could determine positioning, which confirmed the feasibility of the displacement sensing mechanism.



(a)



(b)



(c)

Fig. 13. (Color online) Application of the displacement sensor. (a) Experimental setup, (b) displacement sensor, and (c) displacement signal.

4. Conclusions

Novel bend-type electrodes for enhancing the sensitivity of piezoelectric sensing elements were designed, adopting screen printing technology to produce the electrodes. The bend-type sensing element induced an average positive voltage of 960.5 mV under a tapping experiment, providing a 59.74% increase in maximum voltage compared with a standard series-type sensing element. A prototype displacement sensor using the bend-type sensing element was also tested, verifying the feasibility of the design.

Acknowledgments

The authors would like to thank the Ministry of Science and Technology (MOST) and Fisheries Agency, Council of Agriculture (FA.COA) for their support to the project [Grant Nos. MOST 107-2218-E-006-031-, MOST 107-2218-E-110-004- and 107AS-14.2.7-FA-F1(3)]. Additionally, this research was, in part, supported by the Ministry of Education, Taiwan, and the Headquarters of Advancement to the Intelligent Manufacturing Center (iMRC), National Cheng Kung University (NCKU).

References

- 1 J. Pu, X. J. Yan, Y. D. Jiang, C. Chang, and L. W. Lin: *Sens. Actuators, A* **92** (2010) 131. <https://doi.org/10.1016/j.sna.2010.09.019>
- 2 C. Chang, V. H. Tran, J. Wang, Y. K. Fuh, and L. W. Lin: *Nano Lett.* **10** (2010) 726. <https://doi.org/10.1021/nl9040719>
- 3 Z. L. Wang and J. Song: *Science* **312** (2006) 242. <https://doi.org/10.1126/science.1124005>
- 4 Y. Qin, X. Wang, and Z. L. Wang: *Nature* **451** (2008) 809. <https://doi.org/10.1038/nature06601>
- 5 R. Yang, Y. Qin, C. Li, G. Zhu, and Z. L. Wang: *Nano Lett.* **9** (2009) 1201. <https://doi.org/10.1021/nl803904b>
- 6 Z. M. Huang, Y. Z. Zhang, M. Kotaki, and S. Ramakrishna: *Compos. Sci. Technol.* **63** (2003) 2223. [https://doi.org/10.1016/S0266-3538\(03\)00178-7](https://doi.org/10.1016/S0266-3538(03)00178-7)
- 7 D. Sun, C. Chang, S. Li, and L. Lin: *Nano Lett.* **6** (2006) 839. <https://doi.org/10.1021/nl0602701>
- 8 W. A. Yee, M. Kotaki, Y. Liu, and X. Lu: *Polymer* **48** (2007) 512. <https://doi.org/10.1016/j.polymer.2006.11.036>
- 9 B. J. Hansen, Y. Liu, R. Yang, and Z. L. Wang: *ACS Nano* **4** (2010) 3647. <https://doi.org/10.1021/nn100845b>
- 10 J. Chang and L. Lin: *Proc. 2011 16th Int. Solid-State Sensors, Actuators and Microsystems Conf. (IEEE, 2011)* 747–750. <https://doi.org/10.1109/TRANSDUCERS.2011.5969865>
- 11 Z. H. Liu, C. T. Pan, Z. Y. Ou, and W. C. Wang: *IEEE Sens. J.* **13** (2013) 4098. <https://doi.org/10.1109/JSEN.2013.2278739>
- 12 C. T. Pan, K. C. Tsai, Y. P. Sun, and C. K. Yen: *Sens. Mater.* **29** (2017) 511. <https://doi.org/10.18494/SAM.2017.1533>
- 13 G. Taylor: *Proc. R. Soc. London, Ser. A* **313** (1969) 453–475. <https://doi.org/www.jstor.org/stable/2416488>

About the Authors



Yi-Cheng Chen received his B.S. and M.S. degrees in mechanical engineering from National Yunlin University of Science and Technology, Yunlin, Taiwan, in 2001 and 2003, respectively. He is currently pursuing his Ph.D. degree in systems and naval mechatronic engineering from National Cheng Kung University, Tainan, Taiwan. He is also currently the Deputy Division Director for Research of the Smart Microsystems Technology Center (MSTC) of the Industrial Technology Research Institute (ITRI). His current research interests focus on photoelectric sensors and their applications to position-sensing systems, location tracking systems, and 3D geometric measurements. (Benson_Chen@itri.org.tw)



Chih-Kun Cheng was born in January 1963 in Tainan, Taiwan. He received his B.S. degree in industrial education and graduated from National Taiwan Normal University in 1987. He received M.S. degree in electrical engineering, National Cheng Kung University, in 1999, and presently in the Ph.D. Program of the Department of Electrical Engineering, National Cheng Kung University. Now, he is the chairperson in the Department of Electrical Engineering, Far East University, Tainan, Taiwan. He has joined the transformer research group since his master thesis research. His major interests are transformer technology, power system, and electric machinery. (n2888122@yahoo.com.tw)



Sheng-Chih Shen received his B.E. and M.S. degrees in automatic control engineering from Feng Chia University, Taiwan, in 1996 and 1998, respectively. He received his PhD degree in 2002 from the Department of Engineering and System Science of National Tsing Hua University in Hsinchu, Taiwan. He was a researcher in the MEMS Division of the Industrial Technology Research Institute (ITRI) from 2002 to 2007, and a visiting scholar in the field of MEMS at Carnegie Mellon University from 2004 to 2005. He joined the Department of Systems and Naval Mechatronic Engineering, National Cheng Kung University, Tainan, Taiwan, as a professor in 2018. His current research interests focus on PVDF fiber sensor, LED fishing lighting, and underwater optic lighting. (scshen@mail.ncku.edu.tw)